Useful information brought from wearable devices to the clinical walk tests in stroke patients

Shao-Li Han[1,2], Min-Chun Pan[1], Toko Sugiharto[1]

[1]*National Central University,* [2]*Cathay General Hospital (Taiwan)*

INTRODUCTION

Stroke has been the leading cause of long-term or permanent disabilities in adults. One of the common impairments left after stroke is weak limbs. These weak limbs or trunk can further hinder patients from walking and from returning to their functional status. The application of clinical assessment scales on stroke patients has posed a significant impact on rehabilitation. These items that patients perform poorly are the aspects that they need further training. Besides, the difference between sequential tests is a simple method to monitor patients' training effects. Although most of these scales are easy to be administered in clinical settings, clinical experts cannot get all movement data from a single test. Along with these neuromuscular testing results, the kinematic analysis provides reliable and numeric data for clinical consultants to understand how neuromotor disorder affected stroke patients' abilities. Today, mechanical engineers can embed many sensors into a small module, suitable for wearable devices, to gain movement data from human motion due to the advance of microelectromechanical systems. To establish reliable and accurate algorithms for estimating walking kinematics from these compact devices has been one of the major preoccupations of medical device research in the past decades [1–3]. Although these devices have applied to human motion analysis over the years, only recently has some researchers point how these devices can help clinical assessment scales [4].

Walking tests in stroke patients can give clinical experts many significant functional statuses and even the prognostic predictors. It is a feasible, intuitive, and reliable method in clinical units to obtain functional recovery status in post-stroke patients [5–9]. Over a few decades, there has been much research documenting how sarcopenia affects walking speeds. In short, walking speeds are one of the criteria to diagnose sarcopenia. However, walking speeds among stroke patients are also affected by weak limbs. It is, therefore, straightforward to conclude that stroke patients have a higher risk of getting sarcopenia [10]. Several methods have been proposed to obtain kinematics through wearable devices nowadays [11]. They are promising but challenging, such as obtaining accurate spatiotemporal data, integrating with several sensors, and other transmission issues[12]. Applying wearable devices, primarily composed of inertial measurement units in patients with neurological disorders, exist in some estimating errors in spite of their excellent performance in healthy participants [13]. One of the debating issues is integrating errors from inertial measurement units. Saremi and Marehbian note that walking speed and temporal data is less reliable in stroke with slow walking speeds (<0.5 m/s) [14].

To sum up, the walking speed test is a clinically useful tool to evaluate patients' functional status but there still exist kinematics that has impact on walking speeds. By using IMUs, there still exists challenges. There have been several advantages and disadvantages when either adopting wearable devices alone or clinical assessment scales alone. Another attractive topic is where and how many wearables needed to obtain enough kinematics for clinical application. Integrating wearable devices with clinical assessment scales should be the intuitive and workable method to overcome those shortages. The purpose of this research focuses on setting up a wearable system and managing to integrate clinical walk tests. This hybrid method is supposed to acquire kinematics among walkable stroke patients through wearable devices and to determinate the most critical location to provide additional data during walking tests.

MATERIAL AND METHODS

IMU Measurement Module

To get all the gait parameters, we design a wireless inertial sensing device consisting of a sensing module, a control module, a wireless transmission module, a user interface, and a calculation algorithm. Each device consists of the SparkFun 9Dof Razor IMU M0 module that contains IMU sensor MPU-9250 and microprocessor SAM D21, BlueSMiRF Silver Bluetooth module, and 850mAh Lithium polymer battery. A 3D printer constructs the box with polylactic acid filament material. The size of the box is 7 cm x 5.1 cm x 2.2 cm, and the total weight of this module is 38 grams. In this study, we program the user interface by the software, LabVIEW, provided by National Instrument. The user interface is used to control and monitor the devices. This program can calibrate devices and control where and when to start to store data. This interface can handle these four wireless IMU devices and receive array data simultaneously from all the four devices. Besides, this interface includes several control buttons and twelve graph columns that can demonstrate real-time three-axis data from the four accelerometers, the four gyroscopes, and the four magnetometers. To estimate angular displacement from IMUs is difficult. We adopt the so-called “the Madgwichk algorithm” [15].

IRB 120 Robot Trajectory Validation

To get the good standard, this research also used ABB robot type IRB 120 for validation. ABB robot can produce an end effector trajectory. Data of end effector trajectory can be used to validate IMU devices. IMU devices were installed on the robot as shown in Fig. 1. Refer to Fig. 2(b), we used only joints angle of θ1, θ2, θ3, and θ5. Each joint was represented by the angular displacement of IMU in Eqs. (1) to (4).

$$\theta_1 = -\theta_{1,z} \quad (1)$$

$$\theta_2 = \theta_{2,y} \quad (2)$$

$$\theta_3 = \theta_{3,y} - \theta_2 \quad (3)$$

$$\theta_5 = \theta_{4,y} - \theta_2 - \theta_3 \ , \quad (0)$$

where $\theta_{1,z}$ is angular displacement of IMU1 in z-axis, $\theta_{2,y}$ is angular displacement of IMU2 in y-axis, $\theta_{3,y}$ is angular displacement of IMU3 in y-axis and $\theta_{4,y}$ is angular displacement of IMU4 in y-axis.

The forward kinematic algorithm is needed to get end effector point of manipulation robot from each joint angle. Before using forward kinematics, we need to determine Denavit-Hartenberg parameters. Denavit-Hartenberg parameters are parameters of manipulation robot that are defined with Denavit-Hartenberg method to facilitate forward and invers kinematics calculation. Table is Denavit-Hartenberg parameters from ABB IRB120. There is a modification from the parameters (in bold) because robot has been modified on the last joint, shown in Fig. 2 (a).

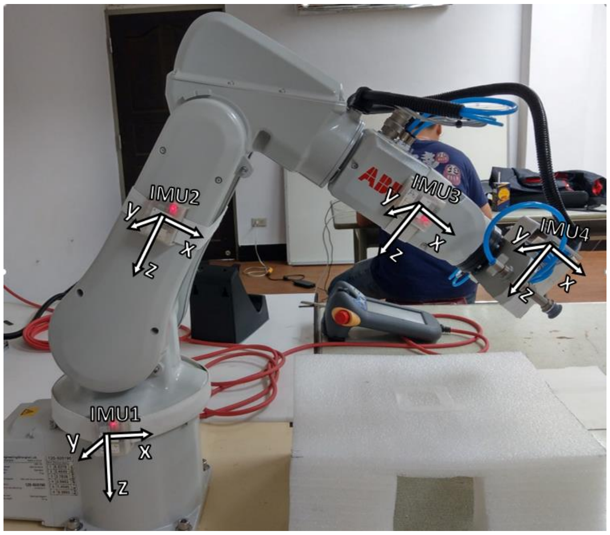

Fig. 1: ABB IRB120 with IMUs position

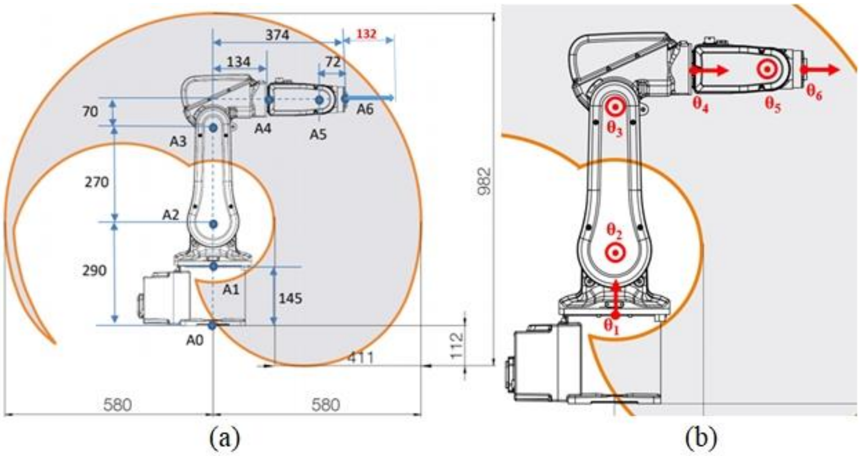

Fig. 2: (a)Size specification (b)Joints rotation of ABB IRB120

Table 1: Denavit-Hartenberg parameters of ABB IRB120 with modification

i	d_i(mm)	θ_i (rad)	a_{i-1}(mm)	α_{i-1} (rad)
1	290	$\boldsymbol{\theta_1}$	0	0
2	0	$\boldsymbol{\theta_2}$ -π/2	0	-π/2
3	0	$\boldsymbol{\theta_3}$	270	0
4	302	θ_4	70	-π/2
5	**100**	$\boldsymbol{\theta_5}$	0	π/2
6	72**+132**	θ_6 +π/2	0	-π/2

To simplify calculation end effector point of the manipulator (forward kinematics algorithm), we need to use Denavit-Hartenberg transformation matrix Eq. (5). Components that used in the matrix are from Table . The transformation matrix will calculate position coordinate of joint *i* from joint *i-1*. If the robot has several joints, an end effector of the robot can be calculated by multiplication of transformation matrix sequentially, as Eq. (6). The end result of multiplication matrix is in Eq. (7). From matrix in Eq. (7), we can get coordinate information of end effector to refer to robot's origin (P_x, P_y, P_z).

$$ {}^{i-1}_{\ \ i}T = \begin{bmatrix} \cos\theta_i & -\sin\theta_i & 0 & a_{i-1} \\ \sin\theta_i\cos\alpha_{i-1} & \cos\theta_i\cos\alpha_{i-1} & -\sin\alpha_{i-1} & -\sin\alpha_{i-1}d_i \\ \sin\theta_i\sin\alpha_{i-1} & \cos\theta_i\sin\alpha_{i-1} & \cos\alpha_{i-1} & \cos\alpha_{i-1}d_i \\ 0 & 0 & 0 & 1 \end{bmatrix} \tag{5} $$

$$ {}^{0}_{N}T = {}^{0}_{1}T\ {}^{1}_{2}T\ {}^{2}_{3}T \ldots {}^{N-1}_{\ \ N}T \tag{6} $$

$$ {}^{0}_{N}T = \begin{bmatrix} r_{11} & r_{12} & r_{13} & P_{x,0} \\ r_{21} & r_{22} & r_{23} & P_{y,0} \\ r_{31} & r_{32} & r_{33} & P_{z,0} \\ 0 & 0 & 0 & 1 \end{bmatrix}. \tag{7} $$

ABB robot can only produce trajectory with the frequency 10 Hz for each point, while in this experiment, we used sampling frequency 100 Hz and 50 Hz. So before validating the trajectory, IMU trajectory data was sampled with interval 100 ms (downsampling). To evaluate the performance of the algorithm, the root means square error (*RMS*) and error percentage were given by Eq. (8) and Eq. (9), where x_i, y_i, and z_i denote the end effector position from IMU's calculation and $x_{i,id}$, $y_{i,id}$, and $z_{i,id}$ denote the end effector positions that were produced by ABB robot. x_c , y_c and z_c are the center point of actual robot trajectory Eq. (10). The distance between center to the ideal point is chosen as error percentage comparator in order to be fairer because trajectory motion is far from the origin point of the ABB robot.

$$ Error_{RMS} = \sqrt{\frac{1}{N}\sum_{i=1}^{N}\left\{\left(x_i - x_{i,id}\right)^2 + \left(y_i - y_{i,id}\right)^2 + \left(z_i - z_{i,id}\right)^2\right\}} \tag{8} $$

$$ Error_{Percentage} = \frac{Error_{RMS}}{\frac{1}{N}\sum_{i=1}^{N}\sqrt{\left(x_{i,id} - x_c\right)^2 + \left(y_{i,id} - y_c\right)^2 + \left(z_{i,id} - z_c\right)^2}} \tag{9} $$

$$ x_c = \frac{\sum x_{i,id}}{N}\ ;\ y_c = \frac{\sum y_{i,id}}{N}\ ;\ z_c = \frac{\sum z_{i,id}}{N} \tag{10} $$

Two motion types are designated to verify the trajectory reconstruction algorithm. Motion 1 mimics the motion of leg in the gait cycle [16]. Joint of θ_1 produced angle as hip angle, θ_3 as knee angle and θ_5 as ankle angle. The motion pattern of flexion angle is divided into 10 movement steps defined in Table. The motion repeated in three times. So in this motion would generate trajectory in two dimensions. In the motion 2, ABB robot rotated with the trajectory in three dimensions with the angle motion each joint is defined in

Table . Purpose of this motion was only to get trajectory in three dimensions of ABB robot to evaluate trajectory that would be generated by wireless IMU system.

Clinical application on walking speeds

The first IMU is affixed directly on subjects' low back, about the level of their fifth vertebrates. We secured the second IMU on their lateral thigh, the third one on their lateral calf, and the fourth one on their dorsum of feet. All IMUs are fastened firmly by Velcro, as illustrated in Fig. 3 for the four IMUs. After wearing the four IMUs, participants receive a 6-meter walk test on flat terrain.

In the beginning, participants sit on the chair; then, they stand up by themselves after getting the hint to start. After balancing well from sitting, they begin to walk at a comfortable speed. The designed computer program has the function to mark the time manually when they go through the start and stop recording points. They repeat consecutively for four times after enough rest. The start point for a 6-meter test is the third meter after they start to walk, and the distance to stop recording is the eighth meter from the outset.

Table 2: Joints angle rotation of motion 1

	Joint θ_1	Joint θ_2	Joint θ_3	Joint θ_4	Joint θ_5
1	0	30	0	0	0
2	0	20	15	0	-5
3	0	10	10	0	0
4	0	-5	0	0	5
5	0	-15	0	0	10
6	0	-20	15	0	0
7	0	-10	35	0	-25
8	0	10	50	0	-15
9	0	25	40	0	0
10	0	30	10	0	5

Table 3: Joints angle rotation of motion 2

	Joint θ_1	Joint θ_2	Joint θ_3	Joint θ_4	Joint θ_5
1	0	30	0	0	0
2	10	20	15	0	-5
3	30	10	10	0	0
4	25	-5	0	0	5
5	0	-15	0	0	10
6	-20	-20	15	0	0
7	-30	-10	35	0	-25
8	-20	10	50	0	-15
9	-5	25	40	0	0
10	0	30	10	0	5

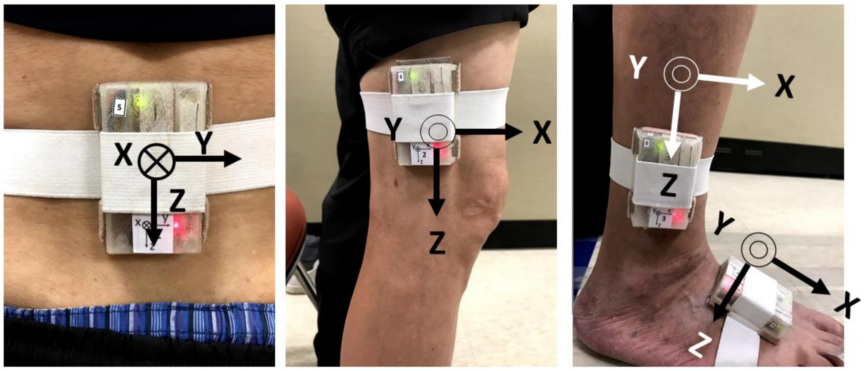

Fig 3. The locations and orientations of the four IMUs.

Subjects and Materials

In the beginning, participants sit on the chair; then, they stand up by themselves after getting the hint to start. After balancing well from sitting, they begin to walk at a comfortable speed. The designed computer program has the function to mark the time manually when they go through the start and stop recording points. They repeat consecutively for four times after enough rest. The start point for a 6-meter test is the third meter after they start to walk, and the distance to stop recording is the eighth meter from the outset.

Clinical application on walking speeds

We recruited walkable adult patients with stable neurological recovery after stroke for longer than one month. Those who cannot follow orders, with recurrent strokes or any surgery in their low limbs before, fall within six months before taking part in this study are exclusive. We also exclude participants who received botulinum injection in lower extremity within six months. All participants received a serial of neuromuscular assessments for stroke, including the Fugl-Meyer assessment scale for lower extremity, Berg balance scale, Postural Assessment after Strokes, and so on to evaluate their disabled status.

Before attending the test, they walk for a short distance to warm up. Then, we secured four IMUs on the participants. After that, all participants stand up, balance well, and start to walk for 10 meters, stop, turned around, and sit again to complete a trial. Subjects are asked to complete four consecutive trials. They walk at a comfortable speed, which they can walk independently with or without any walking devices. Figure 4 gives an example for the computed angular displacement.

RESULTS

There are twenty-five participants recruited in walking tests. There are twenty males and three females. The average of age is 51-year-old. The average body height is 160.5 cm and the average body weight is 74.3 kgs. All participants are right-handed. There are ten subjects with right limbs affected and thirteen with left limbs affected. The results of the Fugl-Meyer assessment for lower extremity read from the lowest eleven to the highest twenty-six. These scores hint their disability level in walking ranged from high walking function to lower walking function. All subjects were consistent with dysfunction left in their lower limbs [17]. There was one subject that completed only three tests because of fatigue in his fourth test.

The four IMUs were fastened at different locations and therefore, the average walking speeds were tested for validity. To test intraclass correlation, a single-rating, absolute-agreement, and 2-way mixed-effects model were adopted. All the walking speed results estimated from these four IMUs revealed excellent coefficients, ranging from 0.998–1 [18]. The concurrent validity tests proved that any one of IMUs in this study can estimate the average walking speeds correctly. The four IMUs in this study can also count steps well. Accordingly, the IMU affixed on the back is the most useful one to obtain additional kinematics during walk tests.

The trajectory range of motion in each joint during walking read little relationship with average comfortable walking speeds. The Pearson's correlation result is listed in the Table 4. The other kinematics are all tested but only moderate correlation of hip range of motion along coronal plane own moderate correlation with average walking speeds. The result is listed in the Table 5.

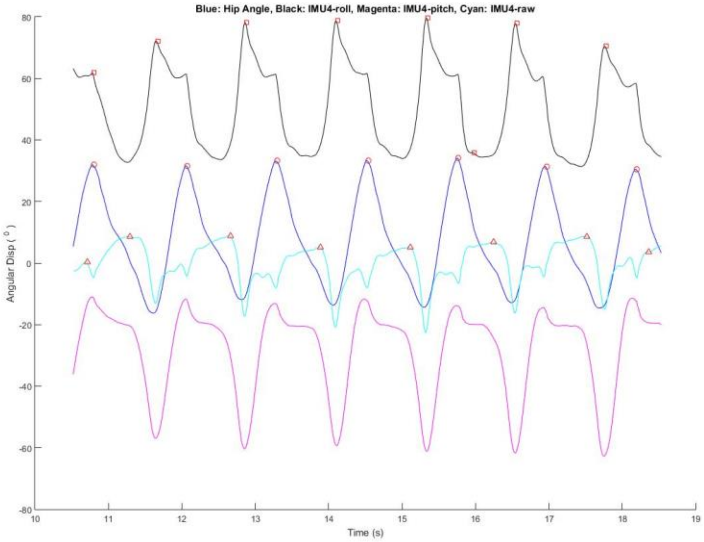

Fig. 4 Computed angular displacement of hip and IMU4 (dorsum of feet).

Table 4. The Correlation results of average trajectory range of motion in each leg joints and average walking speeds

Trajectory range of motion	Correlation results with average walking speeds
Hip	0.231852
Knee	-0.01578
Ankle	0.060535
Summation of three joints	-0.00598

Table 5. The correlation results of average walking speeds and the three-dimensional trajectory ranges of motion from the IMU located on the back.

Trajectory range of motion	Results
Along sagittal plane	-0.23655563
Along coronal plane	-0.464260111*
Along transverse plane	-0.23647188

* Moderately correlated

CONCLUSION

To sum up, a wearable device can add additional kinematic data to the clinical walk test. The IMU attached to the midline of back at the level of the fifth lumbar vertebrae can provide kinematics, including step counts, average step length, cadences, the 3-dimensional angular displacements occurring in the pelvis during walking. The rotational range of motion along coronal planes also has a moderate relationship with comfortable walking speeds. This hybrid module can be a workable and useful guide for rehabilitation in stroke patients.

REFERENCES

[1] Jiang, Gholami, Khoshnam, Eng, andMenon, "Estimation of Ankle Joint Power During Walking Using Two Inertial Sensors," Sensors, vol. 19, no. 12, p. 2796, 2019.

[2] R.Caldas, M.Mundt, W.Potthast, F.Buarque De Lima Neto, andB.Markert, "A systematic review of gait analysis methods based on inertial sensors and adaptive algorithms," Gait Posture, vol. 57, pp. 204–210, 2017.

[3] D.Jarchi, J.Pope, T. K. M.Lee, L.Tamjidi, A.Mirzaei, andS.Sanei, "A Review on Accelerometry-Based Gait Analysis and Emerging Clinical Applications," IEEE Rev. Biomed. Eng., vol. 11, no. c, pp. 177–194, 2018.

[4] V.Cimolin et al., "Do wearable sensors add meaningful information to the Timed Up and Go test? A study on obese women," J. Electromyogr. Kinesiol., vol. 44, no. November 2018, pp. 78–85, 2019.

[5] C.-L.Chen, H.-C.Chen, S. F.-T.Tang, C.-Y.Wu, P.-T.Cheng, andW.-H.Hong, "Gait performance with compensatory adaptations in stroke patients with different degrees of motor recovery.," Am. J. Phys. Med. Rehabil., vol. 82, no. 12, pp. 925–35, Dec.2003.

[6] S.Allin, N.Baker, E.Eckel, andD.Ramanan, “Robust Tracking of the Upper Limb for Functional Stroke Assessment,” IEEE Trans. Neural Syst. Rehabil. Eng., vol. 18, no. c, pp. 1–9, 2010.
[7] C. M.Dean, C. L.Richards, andF.Malouin, “Walking speed over 10 metres overestimates locomotor capacity after stroke,” Clin. Rehabil., vol. 15, no. 4, pp. 415–421, 2001.
[8] M. K.Aaslund et al., “A longitudinal study investigating how stroke severity, disability, and physical function the first week post-stroke are associated with walking speed six months post-stroke,” Physiother Theory Pr., vol. 33, no. 12, pp. 932–942, 2017.
[9] K.Bower et al., “Dynamic balance and instrumented gait variables are independent predictors of falls following stroke,” J. Neuroeng. Rehabil., vol. 16, no. 1, pp. 1–9, 2019.
[10] A. S.Ryan, F.M.Ivery, M.C.Serra, J.Hartstein, andC. E.Hafer-Macko, “Sacropenia and Physical Function in Middle-Aged and Older Stroke Sur vivors,” Ach Phys Med Rehabil, vol. 98, no. 3, pp. 495–499, 2017.
[11] S.Bertuletti, U.DellaCroce, andA.Cereatti, “A wearable solution for accurate step detection based on the direct measurement of the inter-foot distance,” J. Biomech., vol. 84, pp. 274–277, 2019.
[12] S.Qiu, Z.Wang, H.Zhao, L.Liu, andY.Jiang, “Using Body-Worn Sensors for Preliminary Rehabilitation Assessment in Stroke Victims with Gait Impairment,” IEEE Access, vol. 6, pp. 31249–31258, 2018.
[13] D.Trojaniello, A.Ravaschio, J. M.Hausdorff, andA.Cereatti, “Comparative assessment of different methods for the estimation of gait temporal parameters using a single inertial sensor: Application to elderly, post-stroke, Parkinson’s disease and Huntington’s disease subjects,” Gait Posture, vol. 42, no. 3, pp. 310–316, 2015.
[14] K.Saremi et al., “Reliability and validity of bilateral thigh and foot accelerometry measures of walking in healthy and hemiparetic subjects,” Neurorehabil. Neural Repair, vol. 20, no. 2, p. 297(9), 2006.
[15] S. O. H.Madgwick, A. J. L.Harrison, andR.Vaidyanathan, “Estimation of IMU and MARG orientation using a gradient descent algorithm,” IEEE Int. Conf. Rehabil. Robot., 2011.
[16] Michael W. Whittle, Gait analysis an Introduction, 4th ed. Chattanooga: Heidi Harrison, 2007.
[17] P. W. H.Kwong andS. S. M.Ng, “Cutoff Score of the Lower-Extremity Motor Subscale of Fugl-Meyer Assessment in Chronic Stroke Survivors: A Cross-Sectional Study,” Arch. Phys. Med. Rehabil., vol. 100, no. 9, pp. 1782–1787, 2019.
[18] T. K.Koo andM. Y.Li, “A Guideline of Selecting and Reporting Intraclass Correlation Coefficients for Reliability Research,” J. Chiropr. Med., vol. 15, no. 2, pp. 155–163, 2016.